ELSEVIER

Chemical Geology 161 (1999) 165–180

CHEMICAL GEOLOGY
INCLUDING
ISOTOPE GEOSCIENCE

www.elsevier.com/locate/chemgeo

Early cenozoic glaciation, antarctic weathering, and seawater $^{87}Sr/^{86}Sr$: is there a link?

James C. Zachos [a,*], Bradley N. Opdyke [b], Terrence M. Quinn [c], Charles E. Jones [d], Alex N. Halliday [e]

[a] *Earth Sciences Department, University of California, 1156 High Street, Santa Cruz, CA 95064-1077, USA*
[b] *Department of Geology, Australian National University, Canberra, ACT 0200, Australia*
[c] *Department of Geosciences, University of South Florida, Tampa, FL 33620, USA*
[d] *Department of Geology, University of North Carolina, Chapel Hill, NC 27599, USA*
[e] *Department of Geological Sciences, University of Michigan, Ann Arbor, MI 48109, USA*

Received 30 July 1998; accepted 20 October 1998

Abstract

Stable and radiogenic isotopic and sedimentological data from sub-Antarctic deep sea sediment cores reveal a temporal link between changes in seawater $^{87}Sr/^{86}Sr$ ratios and major episodes of late Eocene–early Oligocene climate change. The $^{87}Sr/^{86}Sr$ records show two major inflections, one at 38–39 Ma near the middle/late Eocene boundary, followed by another at 33.4 Ma. Similarly, the oxygen isotope, ice-rafted debris, and clay assemblage records indicate two important climatic events: the appearance of alpine glaciers and/or small ice-sheets on Antarctica in the late Eocene at 38–39 Ma, followed by a rapid transition to larger and more permanent temperate ice-sheets in the early Oligocene at 33.4 Ma. Moreover, during the early Oligocene (30–33 Ma) three to four inferred peaks in glacial activity appear to coincide with subtle steps in the $^{87}Sr/^{86}Sr$ record. The coupled variations in climate and seawater Sr isotope ratios during the Eocene/Oligocene imply a strong causal link between the two. Either changes in climate directly influenced patterns of continental weathering and hence seawater chemistry, and/or a tectonic event (e.g., uplift) as reflected in weathering and seawater chemistry triggered relatively abrupt changes in global climate.

Keywords: Early cenozoic glaciation; Antarctic weathering; Seawater

1. Introduction

Variations in $^{87}Sr/^{86}Sr$ during the Cenozoic as recorded in marine carbonates are thought to reflect changes in the flux of Sr from two primary sources, mid-ocean ridge basalts and continental rocks. Fluxes from ridges are dictated largely by rates of high temperature hydrothermal activity at spreading centers. In contrast fluxes from the continents, which are several times greater than those of ridges, are influenced by several factors including the lithology of surficial rocks and the rates of physical and chemical weathering (Palmer and Edmond, 1992). These factors, in turn, are controlled by two processes: tectonic processes which can increase elevation or alter

* Corresponding author. Tel.: +1-831-459-4644; fax: +1-408-459-3074; e-mail: jzachos@es.ucsc.edu

0009-2541/99/$ - see front matter
PII: S0009-2541(99)00085-6

the exposure of rock lithologies, and climate processes which dictate the rate of chemical weathering and solute transport (Stallard, 1995).

One of the more prominent features of the Sr isotope record is the rapid rise in seawater $^{87}Sr/^{86}Sr$ over the last 40 Ma. The exact significance of this rise in terms of tectonism, climate, and weathering has been a focus of debate for at least the past 20 years (see Ruddiman, 1997 and references therein). The most popular hypothesis relates this increase to a gradual change in the intensity of continental weathering brought about by the collision of India with Asia and subsequent uplift of the Tibetan Plateau and Himalayas (Raymo et al., 1988; Richter et al., 1992). Moreover, this tectonic-induced change in weathering intensity has been implicated as the primary cause of late Cenozoic cooling and glaciation. The higher rates of physical weathering caused by uplift are postulated to have enhanced chemical reactions that either consume carbon dioxide and/or release more nutrients to the oceans, thus providing a mechanism for lowering greenhouse gas levels and cooling the Earth's surface (Raymo, 1994; Raymo and Ruddiman, 1992).

Uplift as the primary mechanism for increasing seawater Sr composition over the late Cenozoic is supported by the fact that the two major rivers draining the Himalayan highlands today are responsible for supplying over 25% of the Sr entering the oceans and that $^{87}Sr/^{86}Sr$ of dissolved Sr in these rivers is anomalously high (Edmond, 1992; Palmer and Edmond, 1992). There is reason to suspect, however, that other processes may have contributed to shaping the seawater Sr isotope curve as well as initiating glaciation during the early Cenozoic. For one, although the initial collision and uplift of the Tibetan Plateau occurred as early as the middle-late Eocene (Chung et al., 1998), various lines of evidence point toward the late early Miocene as the period of most rapid uplift and erosion (Harrison et al., 1992). During the period when Sr ratios began to rise, the Himalayas and Tibetan Plateau were still small-scale features and their contribution of sediments as well as radiogenic Sr to the ocean was substantially less than estimated for the last 10 Ma (Rea, 1992; Quade et al., 1997; Rea et al., 1998). Furthermore, on the basis of both theoretical and empirical studies some investigators have questioned key aspects of the proposed silicate weathering — pCO_2 — feedback as a mechanism for climate change. For one, modeling experiments indicate that atmospheric CO_2 levels have been controlled mainly

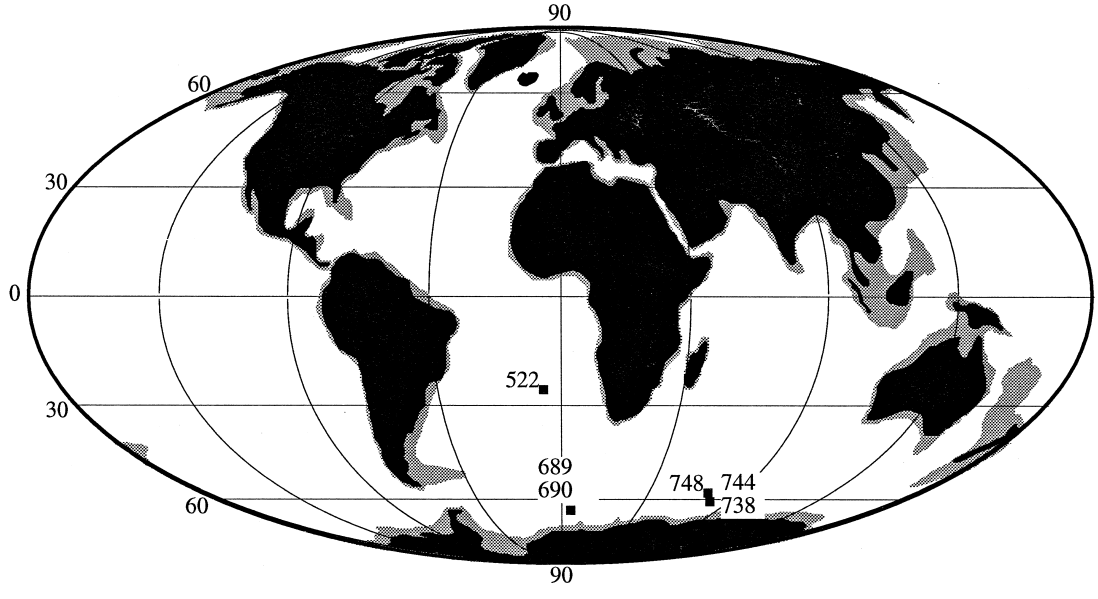

Fig. 1. Map showing the present day locations of DSDP and ODP Sites considered in this study.

by rates of volcanic outgassing and not weathering (Volk et al., 1993). Moreover, field studies show that the primary source of radiogenic Sr and other cations in Himalayan watersheds is not silicate minerals but metalimestones and other carbonates (Palmer and Edmond, 1992; Quade et al., 1997; Blum et al., 1998).

In considering the meaning of the Sr isotope record in this debate, one weathering variable that is often ignored is climate. In the case of the Eocene–Oligocene (E–O) transition, this may be a major oversight. This period is marked by one of the more prominent climate transitions of the last 100 Ma, a transition that included cooling, the appearance of continental ice-sheets on Antarctica, and global shifts in precipitation distribution and intensity. Such a climate event should have had a noticeable impact on regional if not global weathering patterns. In the case of Sr isotopes, the primary changes might have come from effects of ice-sheets exhuming and erod-

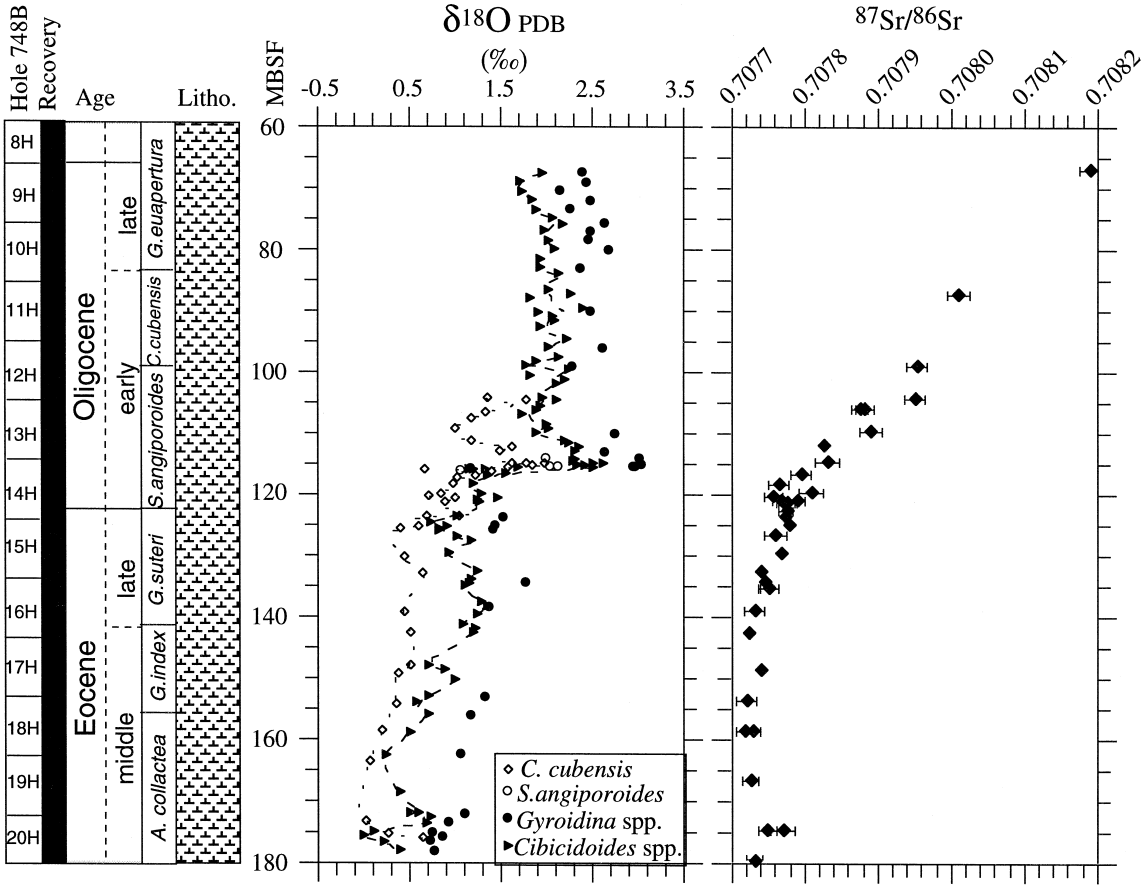

Fig. 2. Site 748 $\delta^{18}O$ and $^{87}Sr/^{86}Sr$ isotopes plotted vs. meters below the sea floor (mbsf). The oxygen isotope records are based on planktonic and benthic foraminifer values (Zachos et al., 1992a,b). The $^{87}Sr/^{86}Sr$ record generated for this study is based on planktonic foraminifer values. Sediment samples were disaggregated in deionized water then washed in 63 μm sieves to rinse away fine particles and sea salts. 30 to 40 specimens were hand picked from the 300–425 μm fraction of each sample and ultrasonically cleaned in methyl alcohol to remove adhering coccoliths. Samples were dissolved in 3 M ultrapure HNO_3, passed through SrSpec™ resin to separate Sr, and analyzed on a VG Sector mass spectrometer closely following the methods outlined in (Quinn et al., 1991). Total procedural blanks were routinely less than 50 pg Sr. Inter-run precision and machine calibration was monitored by analyzing NIST SRM 987 Sr standard. The average for seven values = 0.710244 ± 14.

ing the ^{87}Sr enriched Antarctic continental shield (i.e., Armstrong, 1971; Brass, 1975, 1976). Assuming ice-sheet erosion did at this or any other time play a more significant role in chemical denudation of shields, seawater Sr isotope ratios should exhibit a consistent relationship to episodes of major continental glaciation, particularly during transitions from a globally ice-free to glaciated state. In this regard, the E–O transition is the most recent period for which there is robust evidence of a transition from a prolonged period of ''minimal'' or ice-free conditions (early-middle Eocene) to a full-scale and permanent glacial state. If climate is an important factor in weathering, we should find evidence of coupling between climate and seawater chemistry variability in sediments deposited during this transition.

The principal objective of this paper is to establish in detail the character and timing of large scale changes in Antarctic climate and weathering relative to changes in the seawater $^{87}Sr/^{86}Sr$ record during the Eocene-Oligocene transition. To this end, we have compiled Sr isotope and various proxy climate and weathering records including clay assemblage and benthic foraminiferal oxygen isotope ($\delta^{18}O$) data from a suite of five pelagic cores from the Indian and Atlantic sectors of the Southern Ocean (ODP Sites 689, 690, 738, 744, and 748) (Fig. 1), as well as additional stable isotope data from a mid-latitude site in the South Atlantic (DSDP Site 522). Our composite Sr isotope record consists of published records from Site 689 (Mead and Hodell, 1995) located on Maud Rise in the Atlantic sector of the Southern Ocean and Site 744 (Barrera et al., 1991) on Kerguelen Plateau in the Indian sector. In addition, we have generated a Sr isotope record for the middle Eocene to late Oligocene interval of Site 748 (Fig. 2, Table 1), also located on Kerguelen. The primary rationale for selecting this particular suite of cores is their location; these sites were near enough to directly record Antarctica climate and yet far enough away to retain a pelagic character (Fig. 1). The latter is a critical requirement for developing continuous, high-resolution time series of seawater Sr and O isotope ratios. With the assistance of a simple box model to evaluate the response time of seawater Sr isotope composition to sudden and gradual changes in the isotope ratio of riverine Sr, we also explore the possibility that the early Cenozoic rise in seawater $^{87}Sr/^{86}Sr$ was related to a climate-induced change in chemical weathering patterns, rather than weathering intensity.

Table 1
$^{87}Sr/^{86}Sr$ values of planktonic foraminifers from ODP Site 748

Core	s	interval	Mbsf	Specimen	$^{87}Sr/^{86}Sr \pm 2\sigma$
Hole 748B					
9 H	1	40–44	67.00	Plank. Foram.	0.708190 ± 14
11 H	2	40–44	87.50	Plank. Foram.	0.708010 ± 14
12 H	3	100–102	99.10	Plank. Foram.	0.707953 ± 13
12 H	7	40–44	104.50	Plank. Foram.	0.707950 ± 14
13 H	2	18–22	106.28	Plank. Foram.	0.707882 ± 13
13 H	2	18–22	106.28	Ostracode	0.707876 ± 11
13 H	4	80–84	109.90	Plank. Foram.	0.707890 ± 16
13 H	6	18–22	112.28	Plank. Foram.	0.707824 ± 17
14 H	1	80–84	114.90	Plank. Foram.	0.707830 ± 14
14 H	2	138–142	116.98	Plank. Foram.	0.707796 ± 14
14 H	3	138–142	118.48	Plank. Foram.	0.707763 ± 14
14 H	4	138–142	119.98	Plank. Foram.	0.707808 ± 16
14 H	5	40–44	120.50	Plank. Foram.	0.707757 ± 13
14 H	5	97–101	121.11	Plank. Foram.	0.707788 ± 11
14 H	5	97–101	121.11	Plank. Foram.	0.707766 ± 11
14 H	5	138–142	121.48	Plank. Foram.	0.707771 ± 11
14 H	5	138–142	121.48	Plank. Foram.	0.707775 ± 13
14 H	5	138–142	121.48	Ostracode	0.707776 ± 11
14 H	6	138–142	122.98	Plank. Foram.	0.707774 ± 11
15 H	1	16–20	123.80	Plank. Foram.	0.707772 ± 11
15 H	2	7–11	125.2	Plank. Foram.	0.707784
15 H	2	16–20	125.30	Plank. Foram.	0.707779 ± 11
15 H	3	40–44	127.00	Plank. Foram.	0.707760 ± 14
15 H	5	7–11	129.70	Plank. Foram.	0.707717
15 H	5	16–20	129.80	Plank. Foram.	0.707766 ± 14
15 H	7	16–20	132.80	Plank. Foram.	0.707738 ± 25
16 H	2	18–22	134.61	Plank. Foram.	0.707745 ± 11
16 H	2	100–102	135.43	Plank. Foram.	0.707750 ± 13
16 H	2	100–102	135.43	Ostracode	0.707751 ± 13
16 H	5	40–44	139.33	Plank. Foram.	0.707730 ± 14
17 H	1	18–22	142.78	Plank. Foram.	0.707722 ± 12
17 H	5	18–22	148.78	Plank. Foram.	0.707740 ± 11
18 H	2	40–44	154.00	Plank. Foram.	0.707720 ± 14
18 H	5	100–102	159.10	Plank. Foram.	0.707727 ± 11
18 H	5	100–102	159.10	Plank. Foram.	0.707717 ± 11
19 H	4	96–100	167.10	Plank. Foram.	0.707724 ± 11
20 H	3	80–84	174.90	Plank. Foram.	0.707770 ± 17
20 H	3	100–102	175.10	Plank. Foram.	0.707748 ± 13
20 H	6	96–100	179.60	Plank. Foram.	0.707731 ± 11

2. Timing and magnitude of Antarctic glaciation

The pre-Neogene history of Antarctic glacial activity has been inferred primarily from two lines of

evidence; direct evidence in the form of glaciomarine sediments in cores from the Antarctic margin, and indirect evidence in the form of benthic foraminifera oxygen isotope records from pelagic sequences. The glaciomarine sediment evidence, which includes deposits of waterlain glacial tills, sands, and diamictites, attests to several episodes of expansive continental glaciation during the Oligocene, and several brief and more localized late Eocene glaciations (Fig. 3) (Barrett et al., 1989; Hambrey et al., 1991; Wise et al., 1991; Breza and Wise, 1992). Likewise, the benthic foraminiferal

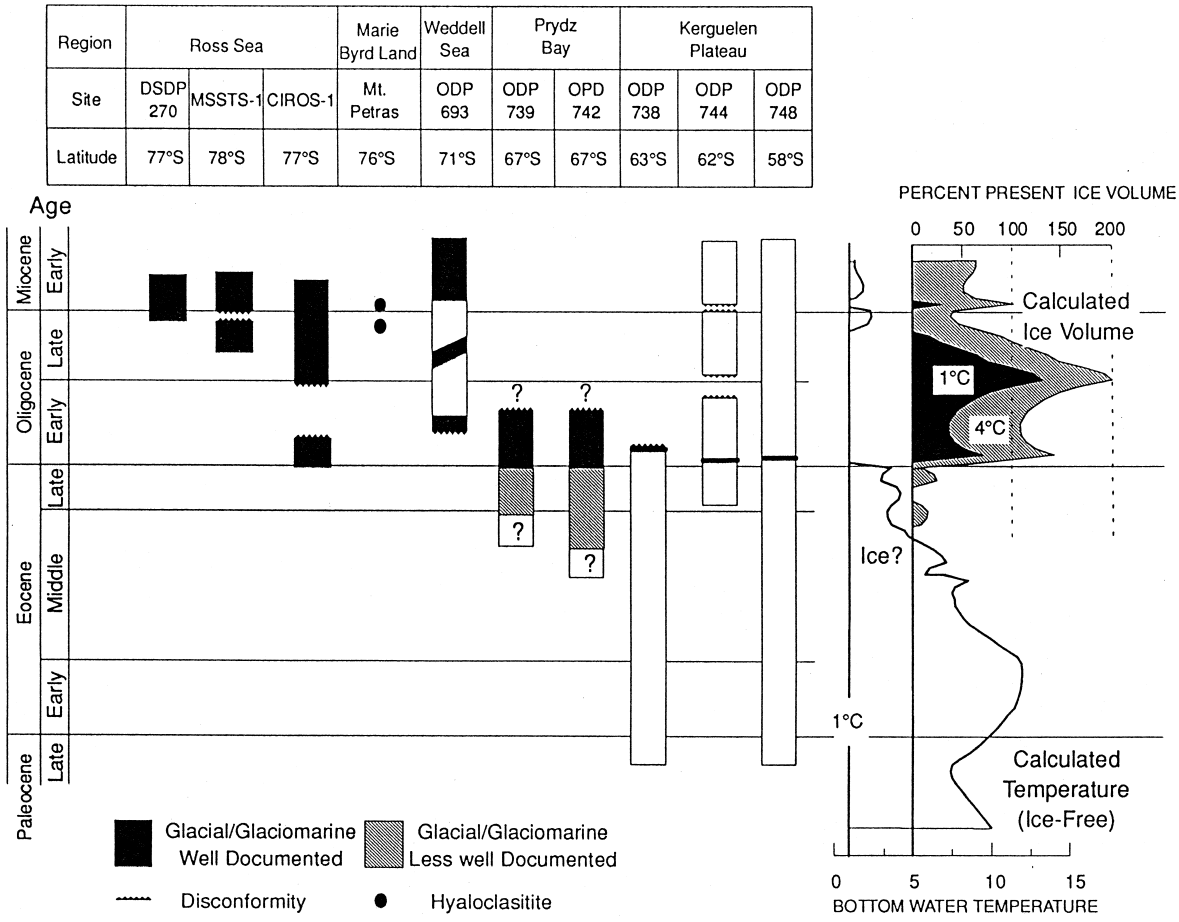

Fig. 3. Plotted to the left is the distribution of well-dated glaciomarine sediments recorded in drill cores from the seas and oceans surrounding Antarctica (Wise et al., 1991). Glaciomarine sediments from Ross Sea and Prydz Bay are comprised mainly of interbedded tills, sand and mudstones (Barrett et al., 1989; Hambrey et al., 1991). Oldest diamictites from Prydz Bay were dated as middle to late Eocene in age. Plotted to the right is an oxygen isotope based reconstruction of Paleogene global ice-volume. The record was constructed using published benthic foraminifer oxygen isotope data (adjusted for disequilibrium vital effects) from 14 DSDP and ODP sites (Zachos et al., 1993) and the calcite/seawater oxygen isotope temperature equation of Erez and Luz (1983). Ice-volumes were calculated as a percentage of present day ice-volume assuming bottom water temperatures of between 1 and 4°C, and a mean isotopic composition for ice of −45‰ (SMOW). The Oligocene ice-volumes computed here exceed those predicted in earlier reconstructions employing similar approaches (Miller et al., 1987). The discrepancy arises mainly from the acquisition of new benthic $\delta^{18}O$ data from southern ocean ODP Sites 744 (Barrera and Huber, 1991), 748 (Zachos et al., 1992a,b), 689 and 690 (Kennett and Stott, 1990) which were located in regions being bathed by colder waters than the low to mid-latitude sites used in earlier reconstructions of early Cenozoic deep sea temperature and ice-volume. Since the range of deep-water temperatures may exceed 5°C, sites closest to the high latitude polar sources of bottom water are required to constrain ice-volume by this approach.

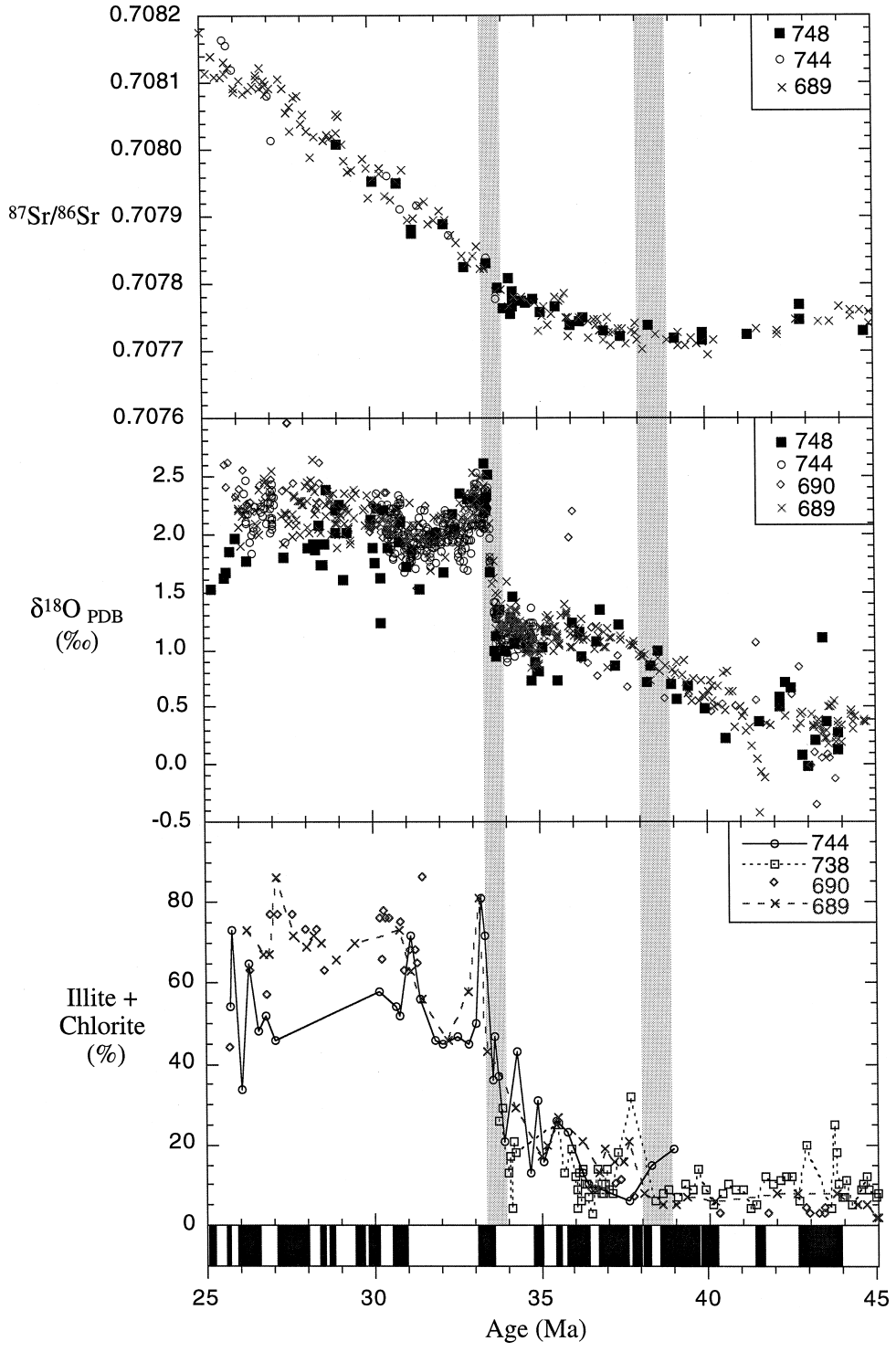
0.7082
0.7081
0.7080
0.7079
0.7078
0.7077
0.7076
87Sr/86Sr
748
744
689
2.5
2.0
1.5
1.0
0.5
0.0
-0.5
δ18O PDB
(‰)
748
744
690
689
80
60
40
20
0
Illite +
Chlorite
(%)
744
738
690
689
25
30
35
40
45
Age (Ma)

oxygen isotope record attests to an extended period of lower deep sea temperature and increased ice-volume beginning in the late Eocene and continuing into the Oligocene (Miller et al., 1987; Zachos et al., 1992a).

To assemble a more detailed picture of E–O glacial activity, we compiled benthic foraminifer $\delta^{18}O$ data from three ODP sites (Fig. 4), 784 (Zachos et al., 1992a,b), 689 (Diester-Haass and Zahn, 1996) and 744 (Zachos et al., 1996). Data from an additional DSDP Site 522 (Zachos et al., 1996) only appear in Fig. 5. The sampling resolution of the records from Sites 689, 744, and 522 (20, 10 and 8 Ka, respectively) is high enough to resolve the middle and lower frequency components (>40 Ka) of orbitally forced changes in climate.

This composite benthic $\delta^{18}O$ record shows several important features including a gradual 0.3‰ increase beginning at ~ 39–41 Ma, a rapid (<150 Ka) >1.2‰ excursion at 33.5 Ma, as well as several small brief excursions at 44, 36, and 29 Ma. The increase at 33.5 Ma is a common feature of all $\delta^{18}O$ records and has been designated Oi-1 (Miller et al., 1991a,b). It most likely represents some combination of global cooling and the appearance of a ''permanent'' full scale ice-sheet on Antarctica (Miller et al., 1987; Zachos et al., 1993, 1996). We stress the term permanent because it is likely that smaller, ephemeral ice-sheets were present during portions of the middle and late Eocene (Barrera and Huber, 1991; Hambrey et al., 1991). One of these potential precursor events is represented by the small positive $\delta^{18}O$ excursion centered at 43 Ma. These and other events from this interval are not well resolved because of hiatuses, poor recovery, and low sampling resolution in existing cores. Another important feature is the pervasive high frequency, low-amplitude oscillations in the Oligocene (Fig. 5). The low-amplitude higher-frequency oscillations are dominated by a cycle with a period near ~ 400 Ka (Fig. 5) (Zahn and Diester-Haass, 1996; Zachos et al., 1996). These are labeled using the alphanumeric scheme of Miller et al. (1991a). Higher-frequency variance, although not well defined, appears to be concentrated at the 41 Ka period (Zachos et al., 1996) suggesting orbital modulation of global ice-volume.

We believe that a substantial portion of the variance (~ 0.4‰) in the deep sea $\delta^{18}O$ record over the Oligocene reflects changes in ice-volume. This inference is based on the following observations: (1) strong covariance between records in different ocean basins suggest that variations in seawater composition rather than temperature are dominating the signal, (2) assuming ice-free conditions, the very high (>2.5‰) benthic $\delta^{18}O$ values for the early Oligocene would require bottom-water temperatures colder than present (Miller et al., 1987; Zachos et al., 1993), and (3) at least three of the positive isotope excursions, at 33.5, 32.6, and 32.0 Ma, have been directly correlated to major sequence boundaries of the New Jersey Margin (Pekar and Miller, 1996). As for the Eocene, with the possible exception of the brief rise at 39 Ma, the role of ice-volume in driving $\delta^{18}O$ variability is less certain.

3. Timing and character of Antarctic continental weathering

As a first-order approximation, the character of continental weathering can be inferred from a small group of primary clays that includes illite, chlorite, smectite, and kaolinite (Chamley, 1990). Illite and chlorite, chemically immature clays, tend to dominate clay assemblages in marine sediments proximal to regions characterized by a high degree of physical weathering and relatively low chemical weathering such as the Antarctic and Arctic. In contrast, smec-

Fig. 4. The upper panel show the strontium isotope values of microfossils from Sites 748 (this study), 744 (Barrera et al., 1992) and 689 (Mead and Hodell, 1995) plotted against age (Ma). The average NIST 987 value reported for the Site 689 data set is 0.710240 ($2s = \pm 0.000022$, $n = 17$). All values were subsequently normalized to NIST-987 = 0.710235. Average values were plotted for those samples at Site 748 with duplicates. The middle panel is composite of benthic foraminifer $\delta^{18}O$ records from Sites 689, 690 (Kennett and Stott, 1990; Diester-Haass and Zahn, 1996), 744 (Zachos et al., 1996), and 748 (Zachos et al., 1992a,b). All values are of benthic taxon *Cibicidoides*. The lower panel shows variations in the % illite + chlorite in sediments for Southern Ocean Sites 738, 744, 689 and 690 (Ehrmann and Mackensen, 1992). These records document a transition from smectite to illite and chlorite-dominated clays beginning at the middle/late Eocene boundary and peaking in the earliest Oligocene. All ages are relative to the GPTS of Cande and Kent (1992).

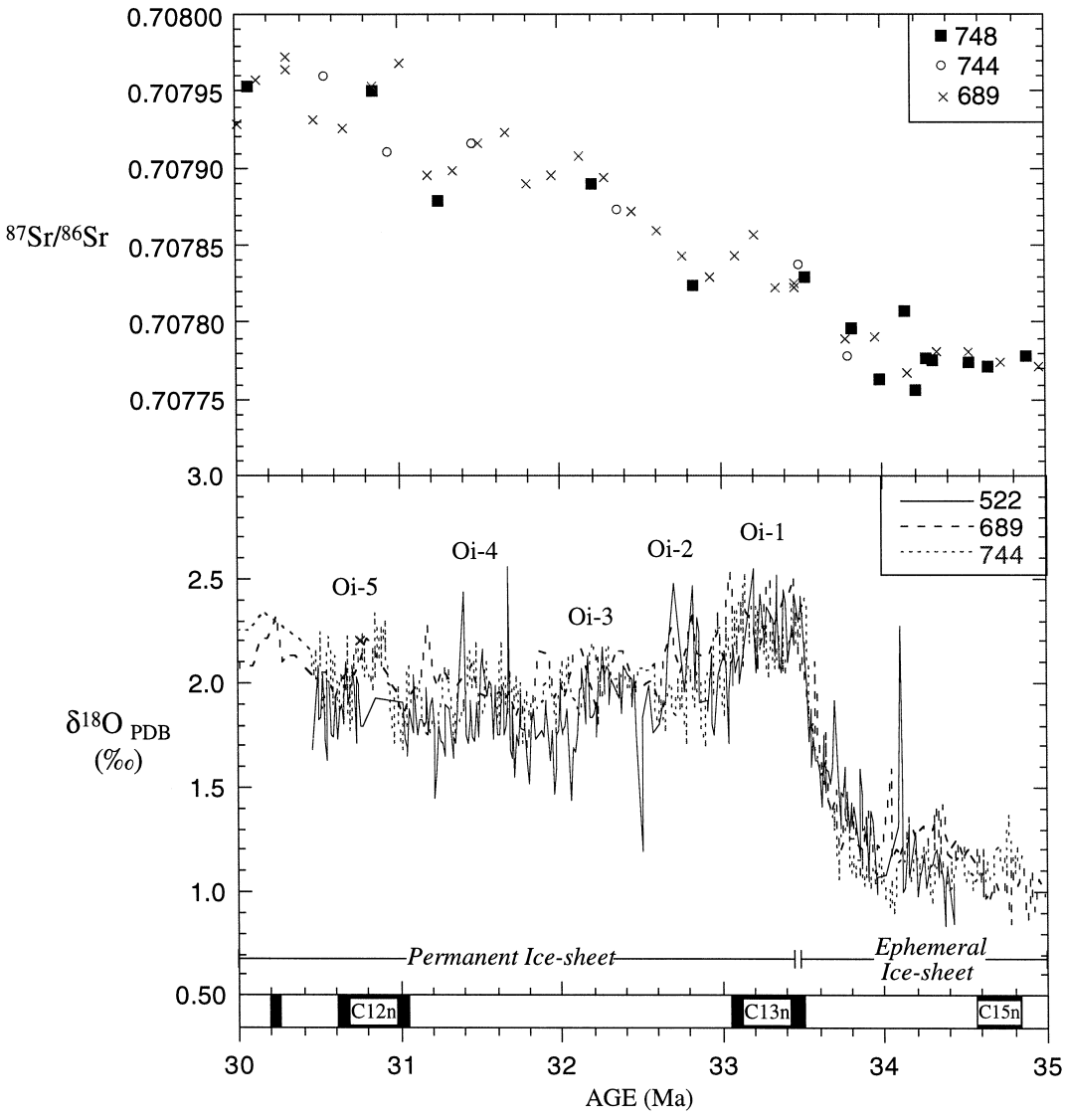

Fig. 5. Comparison of benthic $\delta^{18}O$ (PDB) and seawater $^{87}Sr/^{86}Sr$ from Fig. 4 for the interval 30 to 35 Ma. Benthic $\delta^{18}O$ data are from Sites 522 and 744 (Zachos et al., 1996) and Site 689 (Diester-Haass and Zahn, 1996). Inferred glacial 'maxima' have been labeled using the Oi-designations of Miller et al. (1991a,b). The age model is the same as in previous figures.

tite, a low-temperature chemical alteration product, and kaolinite are more common in low latitude marine sediments proximal to humid regions where runoff is high and soils are chemically mature.

Ehrmann (1991) and Ehrmann and Mackensen (1992) measured the relative concentrations of illite, chlorite, smectite, and kaolinite in Eocene and Oligocene sediments from Sites 689 and 690, and Site 738 and 744. We plotted the combined % illite and % chlorite data alongside our composite isotope figure (the remaining clay is dominated by smectite and essentially shows the reverse pattern). The clay records document a large-scale shift in the character of continental weathering products and clay accumulation in the late Eocene/early Oligocene (Fig. 4). For most of the Eocene, over 80% of the clay

accumulating at Maud Rise and Kerguelen Plateau is smectite. However, beginning in the late Eocene between 38 and 39 Ma, the concentration of illite/chlorite starts to gradually increase. By 33.5 Ma, roughly 60 to 80% of the clay in these cores is illite/chlorite. Moreover, the shift in clay assemblages is accompanied by an increase in the accumulation rate of terrigeneous material on Kerguelen (Salamy and Zachos, 1999).

Assuming the primary source of clays to be the nearest continental land mass, the late Eocene increase in illite–chlorite concentrations across the E/O boundary must reflect an increase in the degree of mechanical weathering (by glaciers) on east Antarctica (Robert and Maillot, 1990; Ehrmann and Mackensen, 1992; Robert and Kennett, 1992). The similarity in magnitude and timing of the clay transition in both Atlantic and Indian sectors of the Southern Ocean argues against this trend reflecting a simple shift in provenance. Furthermore, in the Oligocene, peaks in the illite-chlorite concentrations tend to correspond with peaks in the oxygen isotope record indicating a common link (i.e., ice-sheets). Thus, the record of clay deposition in the southern oceans reinforces the glacial history of Antarctica as inferred from glaciomarine sediment and deep sea oxygen isotope records, specifically that large-scale continental ice-sheets were present on Antarctica by 33.5 Ma. More importantly, the clay proxies constrain the timing of the earliest glacial activity to the middle/late Eocene boundary or roughly 38–39 Ma.

4. Timing of Eocene–Oligocene Sr isotope inflections and steps

The composite Sr isotope stratigraphy for the period 25–45 Ma (Figs. 4 and 5) is based on the Sr isotope ratios of planktonic foraminifera from Sites 748 (Table 1), 744 (Barrera et al., 1991), and 689 (Mead and Hodell, 1995) normalized to NIST SRM 987 standard. We elected not to include the published 522 Sr isotope record (Miller et al., 1988) because of questions concerning preservation of planktonic foraminifera at this site (Mead and Hodell, 1995). Although the majority of data in the composite are from Site 689, essentially every point from Sites 744 and 748 falls on the trend established by the 689 record. This is encouraging and strongly suggests that several of the shorter-term features of the 689 Sr isotope record are reflecting variations in mean seawater composition.

The composite Sr isotope record shows two prominent inflections, one centered at 38–39 Ma and another at 33–34 Ma (Fig. 4). For most of the period preceding the first inflection, Sr ratios are in a gradual decline. Sometime between 38 and 39 Ma, $^{87}Sr/^{86}Sr$ values start to rise at a rate of 1.5×10^{-5}/Ma creating the first inflection. The second inflection is located at 33.4–33.8 Ma, where the rate of increase changes to 5.0×10^{-5}/Ma. Values continue to increase at this rate well into the Oligocene, although the trend appears to be interrupted by a series of steps centered at 33.1, 32.0, 31.3, and 30.8 Ma (Fig. 4). Each step is marked by a slight 0.2–0.3 $\times 10^{-5}$ decline over a period of 200–300 Ka.

5. Discussion

The close correspondence in time between inflections in the seawater Sr isotope record, and prominent transitions in climate at 38–39 Ma and 33–34 Ma provide the most compelling evidence for a link between the two. Either climate was responding to changes in boundary conditions triggered by crustal deformation events (uplift) that also increased the flux of radiogenic Sr to the ocean (i.e., Raymo, 1991; Raymo and Ruddiman, 1992; Richter et al., 1992), and/or episodic high latitude cooling and ice-sheet growth were significantly increasing the mechanical and chemical weathering of continental shield silicates, and hence, the flux of radiogenic Sr to the oceans (e.g., Armstrong, 1971; Oslick et al., 1994).

To better understand the origin of this increase, we designed a simple 1 box model to simulate the effects of an increase in end member Sr isotopic composition of continental riverine input (R_C) on mean ocean $^{87}Sr/^{86}Sr$ (initial ocean value of 0.70775). Two scenarios are simulated, a single ''step'' in which R_C abruptly increases from 0.71108 to 0.71308 and a two step ''ramp'' in which R_C is first increased at a rate of 8.0×10^{-5} Ma^{-1} for the first 5 Ma and then 10.0×10^{-5} Ma^{-1} thereafter. In both scenarios, all Sr fluxes are held constant as are mid-ocean ridge ratios ($R_R = 0.70350$).

The single-step scenario shows an immediate oceanic response with values reaching a plateau at 0.70840 in roughly 10 Ma (Fig. 6a). With the ramp, values also begin to increase immediately but in a more gradual fashion with seawater values rising to 0.70815 over a 15 Ma period (Fig. 6b). The ramped increase fits the observed trend suggesting that the increase in riverine Sr composition and/or fluxes during the Oligocene was gradual, a pattern that could be achieved in one of several ways. Either the exposure and/or weathering rates of more radiogenic Sr increased gradually or it was balanced by a

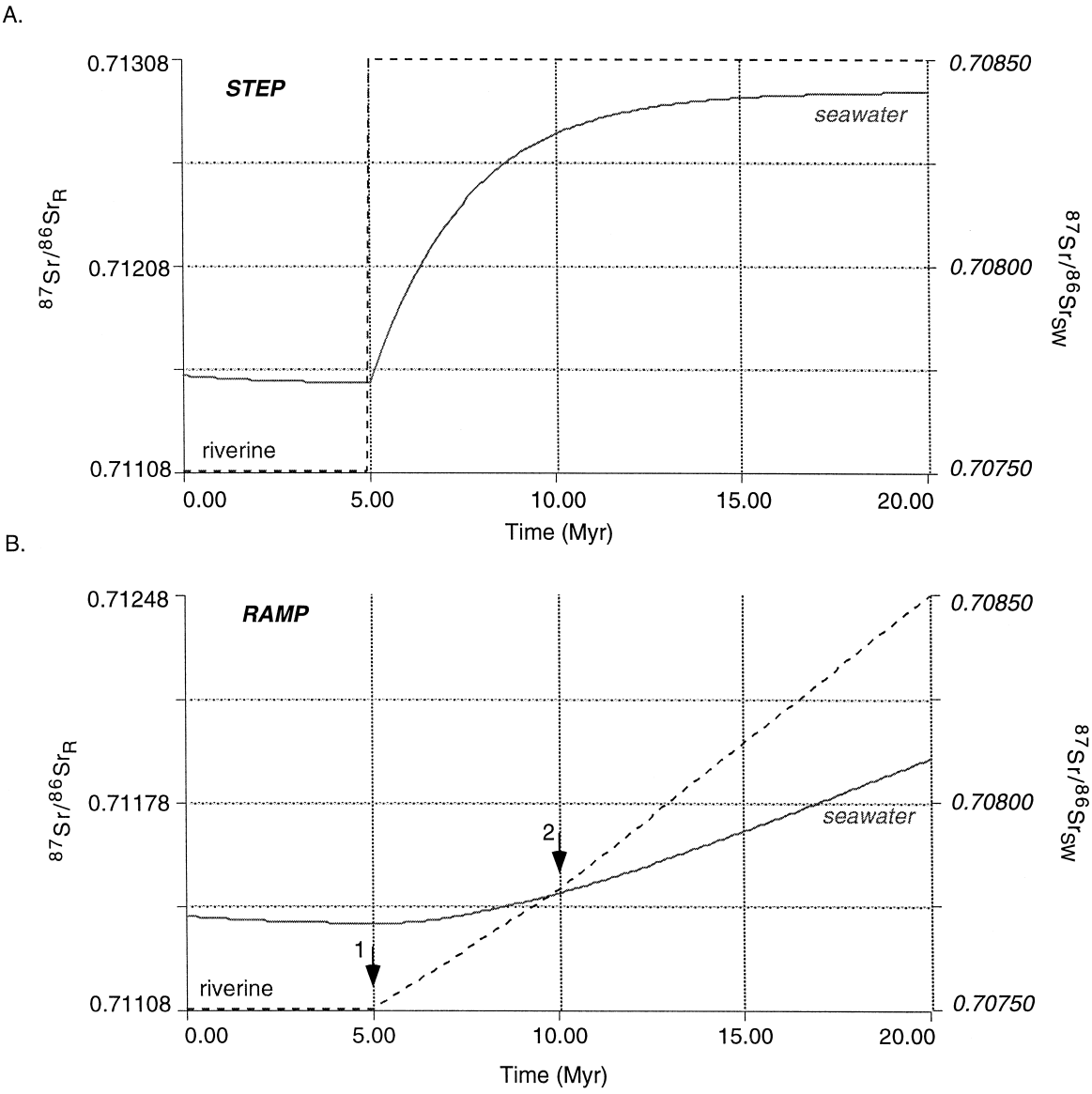

Fig. 6. Results of a simple 1 box modeling exercise designed to simulate the effects on mean ocean $^{87}Sr/^{86}Sr$ of increasing the end-member $^{87}Sr/^{86}Sr$ composition of rivers (R_C) (a) abruptly from 0.71108 to 0.71308 and (b) gradually in a two step 'ramp' (1 and 2) in which R_C is first increased at a rate of 8.0×10^{-5} Ma^{-1} for the first 5 Ma and then 10.0×10^{-5} Ma^{-1} thereafter. In both simulations, all Sr fluxes are held constant as are mid-ocean ridge ratios ($R_R = 0.70350$). The left axis represents river values, the right, seawater values.

gradual decrease in a flux from a less radiogenic source (Richter et al., 1992; Mead and Hodell, 1995). This finding would seem to favor tectonic forcing which is more likely to produce a gradual increase in the flux of Sr to the oceans across the E–O boundary (Hess et al., 1989). Studies of long term cation fluxes to the ocean, however, do not support this simple model. Calcium accumulation in the global ocean serves as a robust cation weathering proxy. Data published with respect to Ca fluxes show an immediate increase in the earliest Oligocene and little change until the early Miocene when fluxes decline, and then resumption of high accumulation rates in the late Miocene (van Andel, 1975; Opdyke and Wilkinson, 1989; Peterson et al., 1992). This record more or less covaries with Antarctic glacial activity suggesting that climate processes were exerting some influence on weathering and marine sediment accumulation during this period.

In addition, as shown in Fig. 5, the rise in seawater Sr during the Oligocene was not smooth but more step-like over relatively short intervals, a pattern that has been observed in other intervals as well (DePaolo and Ingram, 1985; Hodell et al., 1989; Capo and DePaolo, 1990; Miller et al., 1991b; Oslick et al., 1994; Clemens and Farrell, 1995). A step-like pattern suggests pulsed or episodic changes in Sr fluxes and/or isotope ratios which is more consistent with a climate control on weathering (ice-sheets operate on time scales of 10^3 years or longer vs. 10^5 years or longer for mountain building) (Hodell et al., 1989, 1990). Assuming a present day inventory for oceanic Sr, an increase in $^{87}Sr/^{86}Sr$ on the order of 5×10^{-5} over a 800 Ka would require a nearly 40% increase in the flux of Sr into the oceans (Capo and DePaolo, 1990). Such an increase in Sr flux, assuming parallel increases in the flux of all cations, would require unreasonably large increases in chemical weathering rates at the expense of the global carbon budget (Hodell et al., 1989, 1990; Volk, 1989; Francois and Walker, 1992). Alternatively, the increase in Sr isotope ratios could be achieved by gradually increasing the end-member ratio for rivers (Hodell et al., 1989). Again, this would occur if the weathering rates of ''ancient'' silicates increased relative to that of ''young'' silicates and carbonates. The $^{87}Sr/^{86}Sr$ of dissolved Sr in rivers draining pre-Cambrian shields are as high as 0.8–0.9 compared to a global mean of 0.71 for other lithologies (Wadleigh et al., 1985; Edmond, 1992; Palmer and Edmond, 1992). Increased mechanical erosion by ice-sheets, particularly following prolonged periods of ''ice-free'' conditions could produce such a change in weathering patterns without necessarily changing overall chemical fluxes (Armstrong, 1971; Brass, 1976; Capo and DePaolo, 1990; Oslick et al., 1994).

A major drawback of this hypothesis is that numerical modeling exercises have repeatedly found the river flux of Sr draining silicate dominated terrains to be too low to significantly impact seawater $^{87}Sr/^{86}Sr$ ratios (e.g., Hodell and Woodruff, 1994). These simulations, however, typically employ parameterizations for riverine dissolved loads that are based on data for modern rivers. This severely limits the overall flux of dissolved ions that can be generated from ''glaciated'' environments in models. One must question whether modern systems can fully characterize the entire range of climate-induced changes in weathering fluxes occurring over geologic time. We suggest, as some recent studies demonstrate, that the character of chemical weathering (fluxes and ratios) of recently glaciated regions changes rapidly over very short-time scales (Blum and Erel, 1995, 1997).

To fully appreciate the impact a glacial climate regimen can have on chemical denudation rates of continents, it is necessary to consider temperature, weathering and transport mechanics, as well as geologic time, all of which influence the rate at, and extent to which continents erode. The perception that chemical weathering rates decline with decreasing temperatures is not supported by either observation or modeling (Bluth and Kump, 1994; Edmond and Huh, 1997). At best, the effects of temperature appear to be ambiguous. On geologic time scales, it appears that chemical weathering is limited more by the availability of weatherable, preferably fresh, rock surfaces. In this regard, ice-sheets/glaciers, in particular, enhance chemical weathering of continental shield rock by first exhuming and eroding shield rock, thereby increasing the surface/mass ratio by several orders of magnitude, a process which may preferentially accelerate the breakdown of certain mineral phases such as biotite that normally would break down very slowly (Anderson et al., 1997). This debris is then deposited in highly porous allu-

vium that allows for rapid flow through of gas-rich water (Reynolds and Johnson, 1972). In addition, glaciers have a tendency to wax and wane on a variety of time scales (annual to orbital) providing a constant supply of freshly fractured rock. This is particularly important in the case of Sr because some ^{87}Sr enriched mineral phases of igneous and metamorphic rocks tend to be very solution susceptible (Blum and Erel, 1995). These findings imply, as empirical data now demonstrate, that both the concentration and isotopic ratio of dissolved Sr in rivers draining some catchments are highest immediately following deglaciation, and decline substantially thereafter (Blum, 1997).

Another factor that is often overlooked is the spatial scale of the chemical weathering effects of ice-sheets. The effects are not limited to the glaciated region itself, but should extend over much greater areas. For example, rivers and wind often redistribute rock flour (loess) over $\sim 10^4$ km^2 at considerable distances from the terminus of glaciers. Also, the effects of enhanced mechanical weathering may extend to periglacial environments where the annual freeze/thaw cycle in areas of permafrost acts both to rapidly expose fresh mineral surfaces to weathering and to transport materials downslope. For example, data recently collected from the upper Lena River in the Russian far east, which drains the early Archean Aldan Plateau, indicates riverine $^{87}Sr/^{86}Sr$ between 0.710 and 0.713 (Huh et al., 1998). These values are typical of rivers draining ancient granites that are not undergoing intense weathering. What is not typical are the high Sr concentrations found in these rivers: up to 3 uM/kg vs. the world average of 0.9 uM/kg or values of < 0.2 uM/kg for rivers draining the recently glaciated Canadian shield (Wadleigh et al., 1985). While these concentrations are not nearly as high as those found in carbonate-dominated drainages, they suggest that despite cold temperatures, glacial and cold climate regimes through mechanical effects will enhance the susceptibility of continental shield rocks to chemical weathering (e.g., Froelich et al., 1992; Edmond and Huh, 1997).

The absolute limiting factor on chemical weathering in any environment, however, is the availability of water. Regardless of mechanical erosion rates, surface area, etc., without at least periodic input of water, chemical reactions will proceed slowly if at all. The present day Antarctic ice-sheet is dry based and stable, undergoing relatively little seasonal or longer-term meltback. As a result, chemical weathering rates on the continent are negligible. Cold, dry based ice-sheets, however, are a relatively recent phenomena, having only been present on Antarctica since the late Miocene (Margolis and Kennett, 1971; Kennett and Barker, 1990). Prior to that time, under the influence of warmer regional temperatures (Stott et al., 1990) and greater precipitation (Barron et al., 1989), the Antarctic ice-sheets were dynamically much different. For one, they were wet based and fast moving with high water discharge rates as is evident from the vast deposits of waterlain tills and diamictites (Barrett et al., 1989; Hambrey et al., 1991; Wise et al., 1991). Second, even at glacial maxima, the ice-sheets only partially covered the continent and, as a result, much of the sediment debris was deposited on land far from the sea. Third, the ice-sheets were probably less stable; waxing and waning in response to orbital forcing much like the Northern Hemisphere ice-sheets during the Pleistocene (Diester-Haass and Zahn, 1996; Zachos et al., 1996, 1997). Periodic deglaciation coupled with high water discharge rates on a seasonal basis would have provided ample opportunity for chemical weathering of glacial tills and soils.

Cyclic advances and retreats of ice-sheets would have two other important effects on riverine chemical fluxes. First, the flux of radiogenic Sr would be pulsed, creating a gradual, but transient, step-like increase in seawater Sr isotope ratios (e.g., Hodell et al., 1989). Second, the sudden glacioeustatic drop in sealevel would expose shelf carbonates thereby providing a large source of highly mobile but less radiogenic Sr (Stoll and Schrag, 1996). This would initially dampen changes caused by increased weathering of silicates (Gibbs and Kump, 1994), a factor not considered in numerical models.

There is at least one other line of evidence, biogenic silica accumulation rates, which indicate an increase in regional chemical weathering of silicates. In deep-sea cores from the southern and equatorial oceans, the E/O transition is marked by a sudden increase in opal concentrations and accumulation rates (Baldauf and Barron, 1990; Ehrmann, 1991; Diester-Haass, 1995). In the southern Indian ocean, the changes in opal accumulation rates were tightly

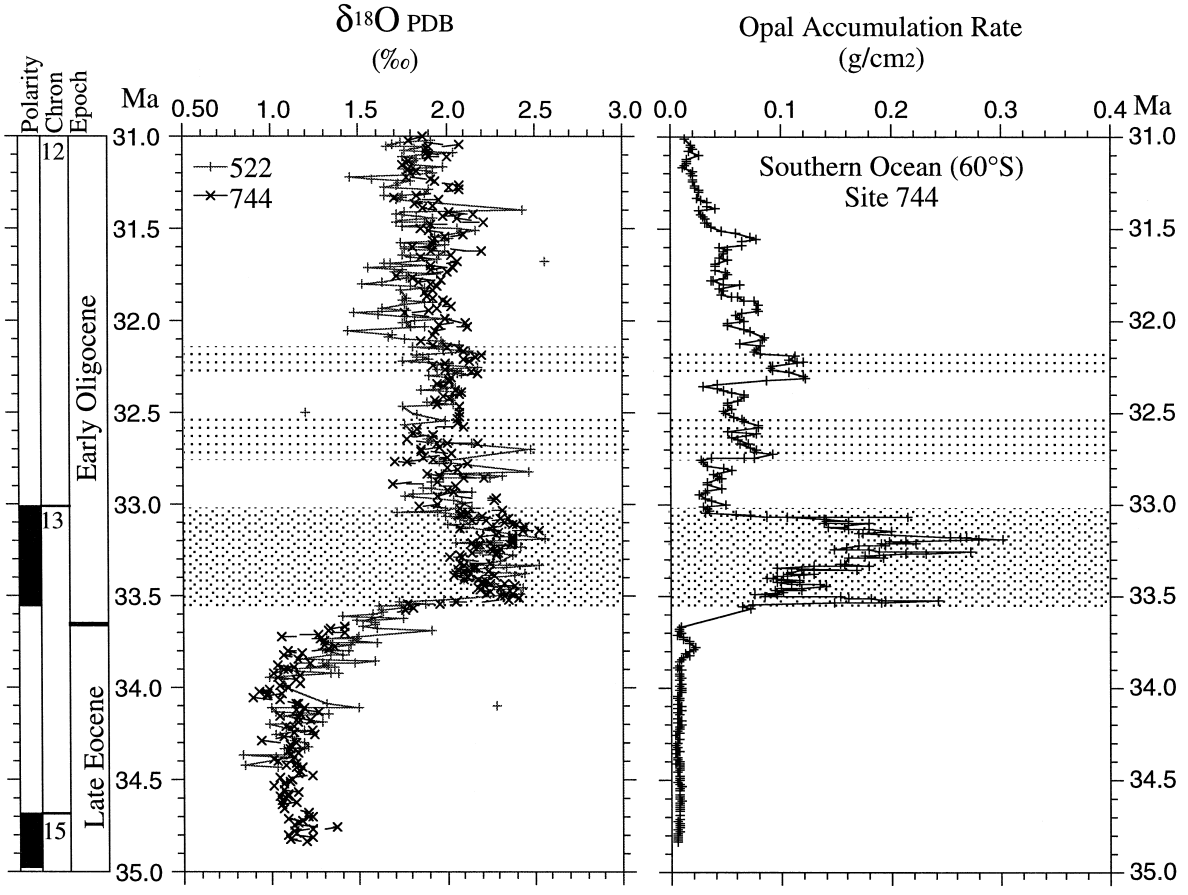

Fig. 7. Site 522 (+) and 744 (×) *Cibicidoides* $\delta^{18}O$ records (Zachos et al., 1996) plotted along with the Site 744 opal accumulation record (Salamy and Zachos, 1999) for the period 31–35 Ma. The age model is the same as in previous figures.

coupled to onset of glacial activity (Salamy and Zachos, 1999). As illustrated in Site 744 sediment cores, opal accumulation rates increased by several orders of magnitude during the Oi-1 transition at 33.5 Ma (Fig. 7). Such a large and rapid change would require an equally rapid but shortlived increase in the supply of dissolved silica to the Southern Ocean, implicating a climatically driven change in chemical denudation patterns.

At present, it is unclear to what extent changes in climate have impacted chemical weathering rates. There is reason to suspect, however, that the chemical weathering of continental rocks, particularly ancient cratonic shields, is strongly climate and time dependent. Weathering in alpine regions would be less so as these environments already experience high rates of physical weathering. Given the dynamic nature of climate and the cryosphere over the Cenozoic, more realistic geochemical models must eventually include the effects of shifting climates on continental weathering patterns (e.g., Bluth and Kump, 1994; Gibbs and Kump, 1994; Sloan et al., 1997).

6. Summary and closing remarks

We recognize that the late Cenozoic rise in seawater $^{87}Sr/^{86}Sr$ was largely driven by erosion changes associated with the uplift of the Himalayas. Isotopic and other records from Southern Ocean deep-sea cores, however, reveal a tight correlation between

shifts in late Eocene and early Oligocene climate and weathering on Antarctica with inflections in the seawater Sr isotope curve at 38–39 and 33–34 Ma. This temporal correlation provides the most compelling evidence for a coupling, either direct or indirect, between the forces that control the ocean Sr budget and global climate. In this paper, we have presented several, largely qualitative arguments as to how a climate induced change in chemical weathering patterns, rather than a change in fluxes, may have contributed to the initial rise in seawater $^{87}Sr/^{86}Sr$ in the early Cenozoic. What is now required are (1) more detailed records of Sr isotope and other geochemical variations during this critical transition in global climate, and (2) a comprehensive set of data specifically focused on weathering of freshly fractured crystalline rock debris immediately following glacial retreat.

Acknowledgements

We thank Karen Salamy and Linda Albertzart for technical assistance. We also thank Lisa Sloan, Suzanne P. Anderson, Rainer Zahn and two anonymous reviewers for their criticisms and comments, and James Kennett, David Hodell, Gabriel Walker, David Rea, Lee Kump, and James Walker for comments on an earlier version (circa 1992) of this manuscript. This research was partially supported by NSF grants OCE-9101861 and OCE-9458367.

References

Anderson, S.P., Drever, J.I., Humphrey, N.F., 1997. Chemical weathering in glacial environments. Geology 25, 399–402.

Armstrong, R.L., 1971. Glacial erosion and the variable isotopic composition of strontium in seawater. Nature 230, 132–134.

Baldauf, J.G., Barron, J.A., 1990. Evolution of biosiliceous sedimentation patterns — Eocene through quarternary: paleoceanographic response to polar cooling. In: Bleil, U., Thiede, J. (Eds.), Geological History of the Polar Oceans, Arctic versus Antarctic. Kluwer, Academic, Norwell, MA, pp. 575–607.

Barrera, E., Huber, B.T., 1991. Paleogene and early Neogene oceanography of the southern Indian Ocean: Leg 119 foraminifer stable isotope results. In: Barron, J., Larsen, B. (Eds.), Proc. ODP, Sci. Results 119, Ocean Drilling Program. College Station, TX, pp. 693–718.

Barrett, P.J., Hambrey, M.J., Harwood, D.M., Pyne, A.R., Webb, P., 1989. Synthesis. In: Barrett, J. (Ed.), Antarctic Cenozoic History from CIROS-1 Drill Hole, McMurdo Sound 245, New Zealand.

Barron, E.J., Hay, W.W., Thompson, S., 1989. The hydrologic cycle; a major variable during Earth history. Global and Planetary Change 1, 157–174.

Blum, J.D., 1997. The effect of Late Cenozoic glaciation and tectonic uplift on silicate weathering rates and the marine $^{87}Sr/^{86}Sr$ record. In: Ruddiman, W.F. (Ed.), Tectonic Uplift and Climate Change. Plenum, New York, NY, pp. 260–289.

Blum, J.D., Erel, Y., 1995. A silicate weathering mechanism linking increases in marine $^{87}Sr/^{86}Sr$ with global glaciation. Nature 373, 415–418.

Blum, J.D., Erel, Y., 1997. Rb–Sr isotope systematics of a granitic soil chronosequence; the importance of biotite weathering. Geochim. Cosmochim. Acta 61, 3193–3204.

Blum, J.D., Gazis, C.A., Jacobson, A.D., Chamberlain, C.P., 1998. Carbonate versus silicate weathering in the Raikhot watershed within the High Himalayan Crystalline Series. Geology 26, 411–414.

Bluth, G.J.S., Kump, L.R., 1994. Lithologic and climatologic controls of river chemistry. Geochim. Cosmochim. Acta 58, 2341–2359.

Brass, G.W., 1975. The effect of weathering on the distribution of strontium isotopes in weathering profiles. Geochim. Cosmochim. Acta 39, 1647–1653.

Brass, G.W., 1976. The variation of the marine $^{87}Sr/^{86}Sr$ ratio during Phanerozoic time; interpretation using a flux model. Geochim. Cosmochim. Acta 40, 721–730.

Breza, J., Wise, S.W., 1992. Lower Oligocene Ice-Rafted Debris on the Kerguelen Plateau: evidence for East Antarctic Continental Glaciation. In: Schlich, R., Wise, S.W. (Eds.), Proc. ODP, Sci. Results 120, Ocean Drilling Program. College Station, TX, pp. 161–178.

Cande, S.C., Kent, D., 1992. A new geomagnetic polarity time scale for the Late Cretaceous and Cenozoic. J. Geophys. Res. 97, 13917–13951.

Capo, R.C., DePaolo, D.J., 1990. Seawater strontium isotopic variations from 2.5 million years ago to the present. Science 249, 51–55.

Chamley, H., 1990. Sedimentology. Springer, New York.

Chung, S.L., Lo, C.H., Lee, T.Y., Zhang, Y., Xie, Y., Li, X., Wang, K.L., Wang, P.L., 1998. Diachronous uplift of the Tibetan plateau starting 40 myr ago. Nature 394, 769–773.

DePaolo, D.J., Ingram, B.L., 1985. High resolution stratigraphy with strontium isotopes. Science 227, 938–941.

Diester-Haass, L., 1995. Middle Eocene to early Oligocene paleoceanography of the Antarctic Ocean (Maud Rise, ODP Leg 113, Site 689): change from low to a high productivity ocean. Palaeogeogr. Palaeoclimatol. Palaeoecol. 113, 311–334.

Diester-Haass, L., Zahn, R., 1996. Eocene–Oligocene transition in the Southern Ocean: history of water mass circulation and biological productivity. Geology 24, 163–166.

Edmond, J.M., 1992. Himalayan tectonics, weathering processes,

and the strontium isotope record in marine limestones. Science 258, 1594–1597.

Edmond, J.M., Huh, Y., 1997. Chemical weathering yields in hot and cold climates. In: Ruddiman, W.F. (Ed.), Tectonic Uplift and Climate Change. Plenum, New York, NY.

Ehrmann, W.U., 1991. Implications of sediment composition on the southern Kerguelen Plateau for paleoclimate and depositional environment. In: Barron, J., Larsen, B., et al. (Eds.), Proc. ODP, Sci. Results 119, Ocean Drilling Program. College Station, TX, pp. 185–210.

Ehrmann, W.U., Mackensen, A., 1992. Sedimentological evidence for the formation of an East Antarctic ice sheet in Eocene/Oligocene time. Palaeogeogr. Palaeoclimatol. Palaeoecol. 93, 85–112.

Erez, J., Luz, B., 1983. Experimental paleotemperature equation for planktonic foraminifera. Geochim. Cosmochim. Acta 47, 1025–1031.

Francois, L.M., Walker, J.C.G., 1992. Modelling the Phanerozoic carbon cycle and climate; constraints from the $^{87}Sr/^{86}Sr$ isotopic ratio of seawater. Am. J. Sci. 292, 81–135.

Froelich, P.N., Blanc, V., Mortlock, R.A., Chillrud, S.N., Dunstan, W., Udomkit, A., Peng, T., 1992. River fluxes of dissolved silica to the ocean were higher during glacials: Ge/Si diatoms, rivers, oceans. Paleoceanography 7, 739–767.

Gibbs, M.T., Kump, L.R., 1994. Global chemical erosion during the last glacial maximum and the present; sensitivity to changes in lithology and hydrology. Paleoceanography 9, 529–543.

Hambrey, M.J., Ehrmann, W.U., Larsen, B., 1991. Cenozoic glacial record of the Prydz Bay Continental Shelf, East Antarctica. In: Barron, J., Larsen, B. et al. (Eds.), Proc. ODP, Sci. Results 119, Ocean Drilling Program. College Station, TX, pp. 77–132.

Harrison, T.M., Copeland, P., Kidd, W.S.F., Yin, A., 1992. Raising Tibet. Science 255, 1663–1670.

Hess, J., Stott, L.D., Bender, M.L., Kennett, J.P., Schilling, J., 1989. The Oligocene marine microfossil record: age assessments using Sr isotopes. Paleoceanography 4, 655–679.

Hodell, D.A., Woodruff, F., 1994. Variations in the strontium isotopic ratio of seawater during the Miocene: stratigraphic and geochemical implications. Paleoceanography 9, 405–426.

Hodell, D.A., Mueller, P.A., McKenzie, J.A., Mead, G.A., 1989. Strontium isotope stratigraphy and geochemistry of the late Neogene ocean. Earth Planet. Sci. Lett. 92, 165–178.

Hodell, D.A., Mead, G.A., Mueller, P.A., 1990. Variation in the strontium isotopic composition of seawater (8 Ma to present): implications for chemical weathering rates and dissolved fluxes to the oceans. Chem. Geol. 80, 291–307, Isotope Geosciences Section.

Huh, Y., Tsoi, M.Y., Zaitsev, A., Edmond, J., 1998. The fluvial geochemistry of the rivers of Eastern Siberia: I. Tributaries of the Lena River draining the sedimentary platform of the Siberian Craton. Geochim. Cosmochim. Acta 62, 1657–1676.

Kennett, J.P., Barker, P.F., 1990. Climatic and Oceanographic developments in the Weddell Sea, Antarctica, since the latest Cretaceous, an ocean-drilling perspective. In: Barker, P.F., Kennett, J.P. (Eds.), Proc. ODP, Sci. Results 113, Ocean Drilling Program. College Station, TX, pp. 937–962.

Kennett, J.P., Stott, L.D., 1990. Proteus and Proto-Oceanus, Paleogene Oceans as revealed from Antarctic stable isotopic results; ODP Leg 113. Proc. ODP, Sci. Results 113, Ocean Drilling Program. College Station, TX, pp. 865–880.

Margolis, S., Kennett, J.P., 1971. Cenozoic paleoglacial history of Antarctica recorded in subantarctic deep-sea cores. Am. J. Sci. 271, 1–36.

Mead, G.A., Hodell, D.A., 1995. Controls on the $^{87}Sr/^{86}Sr$ composition of seawater from the middle Eocene to Oligocene: hole 689B, Maud Rise, Antarctica. Paleoceanography 10, 327–346.

Miller, K.G., Fairbanks, R.G., Mountain, G.S., 1987. Tertiary oxygen isotope synthesis, sea-level history/continental margin erosion. Paleoceanography 2, 1–19.

Miller, K.G., Feigenson, M.D., Kent, D., Olsson, R.K., 1988. Upper Eocene to Oligocene isotope ($^{87}Sr/^{86}Sr$, $\delta^{18}O$, $\delta^{13}C$) standard section, Deep-sea Drilling Project Site 522. Paleoceanography 3, 223–233.

Miller, K.G., Wright, J.D., Fairbanks, R.G., 1991a. Unlocking the ice house: Oligocene–Miocene oxygen isotopes, eustacy, and margin erosion. J. Geophys. Res. 96, 6829–6848.

Miller, K.G., Feigenson, M.D., Wright, J.D., Clement, B.M., 1991b. Miocene isotope reference section, Deep Sea Drilling Project Site 608: an evaluation of isotope and biostratigraphic resolution. Paleoceanography 6, 33–52.

Opdyke, B.N., Wilkinson, B.H., 1989. Surface area control of shallow cratonic to deep marine carbonate accumulation. Paleoceanography 3, 685–703.

Oslick, J.S., Miller, K.G., Feigenson, M.D., Wright, J.D., 1994. Oligocene–Miocene strontium isotopes: stratigraphic revisions and correlations to an inferred glacioeustatic record. Paleoceanography 9, 427–443.

Palmer, M.R., Edmond, J.M., 1992. Controls over the strontium isotope composition of river water. Geochim. Cosmochim. Acta 56, 2099–2111.

Pekar, S., Miller, K.G., 1996. New Jersey Oligocene 'icehouse' sequences (ODP Leg 150X) correlated with global delta ^{18}O and Exxon eustatic records. Geology 24, 567–570.

Peterson, L.C., Murray, D.W., Ehrmann, W.U., Hempel, P., 1992. Cenozoic carbonate accumulation and compensation depth changes in the Indian Ocean. In: Duncan, R.A., Rea, D.K., Kidd, R.B., von Rad, U., Weissel, J.K. (Eds.), Synthesis of Results from Scientific Drilling in the Indian Ocean., Amer. Geophys. Union Geophys. Monogr. 70, 311–333.

Quade, J., Roe, L., DeCelles, P.G., Ojha, T.P., 1997. The late Neogene $^{87}Sr/^{86}Sr$ record of lowland Himalayan rivers. Science 276, 1828–1831.

Quinn, T.M., Lohmann, K.C., Halliday, A.N., 1991. Sr isotopic variation in shallow water carbonate sequences; stratigraphic, chronostratigraphic, and eustatic implications of the record at Enewetak Atoll. Paleoceanography 6, 371–385.

Raymo, M.E., 1991. Geochemical evidence supporting T.C. Chamberlin's theory of glaciation. Geology 19, 344–347.

Raymo, M.E., 1994. The Himalayas, organic carbon burial and climate in the Miocene. Paleoceanography 9, 399–404.

Raymo, M.E., Ruddiman, W.F., 1992. Tectonic forcing of late Cenozoic climate. Nature 359, 117–122.

Raymo, M.E., Ruddiman, W.F., Froelich, P.N., 1988. Influence of late Cenozoic mountain building on ocean geochemical cycles. Geology 16, 649–653.

Rea, D.K., 1992. Delivery of Himalayan sediment to the Northern Indian Ocean and its relation to global climate, sea level, uplift, and seawater strontium. In: Duncan, R.A., Rea, D.K., Kidd, R.B., von Rad, U., Weissel, J.K. (Eds.), Synthesis of Results from Scientific Drilling in the Indian Ocean. Am. Geophys. Union Geophys. Monogr. 70, pp. 387–402.

Rea, D.K., Snoeckx, H., Joseph, L.H., 1998. Late Cenozoic eolian deposition in the North Pacific; Asian drying, Tibetan uplift, and cooling of the Northern Hemisphere. Paleoceanography 13, 215–224.

Reynolds, R.C., Johnson, N.M., 1972. Chemical weathering in the temperate glacial environment of the northern Cascade Mountains. Geochim. Cosmochim. Acta 36, 537–554.

Richter, F.M., Rowley, D.B., DePaolo, D.J., 1992. Sr isotope evolution of seawater: the role of tectonics. Earth Planet. Sci. Lett. 109, 11–23.

Robert, C., Kennett, J.P., 1992. Paleocene and Eocene kaolinite distribution in the South Atlantic and Southern Ocean; Antarctic climatic and paleoceanographic implications. Mar. Geol. 103, 99–110.

Robert, C.M., Maillot, H.B., 1990. Paleoenvironments in the Weddell Sea area and Antarctic climates, as deduced from clay mineral associations and geochemical data, ODP Leg 113. In: Barker, P.F., Kennett, J.P. (Eds.), Proc. ODP, Sci. Results 113, Ocean Drilling Program. College Station, TX, pp. 51–70.

Salamy, K.A., Zachos, J.C., 1999. Late Eocene-early Oligocene climate change on southern ocean fertility: inferences from sediment accumulation and stable isotope data. Palaeogeogr. Palaeoclimat. Palaeoecol. 145, 61–78.

Stallard, R.F., 1995. Tectonic, environmental, and human aspect of weathering and erosion: a global review using a steady-state perspective. Annu. Rev. Earth Planet. Sci. 23, 11–39.

Stoll, H.M., Schrag, D.P., 1996. Evidence for glacial control of rapid sea level changes in the Early Cretaceous. Science 272, 1771–1774.

Stott, L.D., Kennett, J.P., Shackleton, N.J., Corfield, R.M., 1990. The evolution of Antarctic surface waters during the Paleogene; inferences from the stable isotopic composition of planktonic foraminifera. In: Barker, P.F., Kennett, J.P. (Eds.), Proc. ODP Sci. Results 113, Ocean Drilling Program. College Station, TX, pp. 849–864.

Volk, T., Caldeira, K., Arthur, M.A., Berner, R.A., Lasaga, A.C., 1993. Cooling in the late Cenozoic. Nature 361, 123–124, discussions and reply.

Wadleigh, M.A., Veizer, J., Brooks, C., 1985. Strontium and its isotopes in Canadian rivers: fluxes and global implications. Geochim. Cosmochim. Acta 49, 1727–1736.

Wise, S.W., Breza, J.R., Harwood, D.M., Wei, W., 1991. Paleogene glacial history of Antarctica. In: Controversies in Modern Geology, pp. 133–171.

Zachos, J.C., Berggren, W.A., Aubry, M., Mackensen, A., 1992a. Isotope and trace element geochemistry of Eocene and Oligocene foraminifers from Site 748, Kerguelen Plateau. In: Schlich, R., Wise, S.W. (Eds.), Proc. ODP, Sci. Results 120, Ocean Drilling Program. College Station, TX, pp. 839–854.

Zachos, J.C., Breza, J., Wise, S.W., 1992b. Early Oligocene ice-sheet expansion on Antarctica: sedimentological and Isotopic evidence from Kerguelen Plateau. Geology 20, 569–573.

Zachos, J.C., Lohmann, K.C., Walker, J.C.G., Wise, S.W., 1993. Abrupt climate change and transient climates in the Paleogene: a marine perspective. J. Geol. 101, 191–213.

Zachos, J.C., Quinn, T.M., Salamy, K.A., 1996. Earliest Oligocene climate transition: constraints from high resolution (10^4 yr) deep-sea foraminiferal $\delta^{18}O$ and $\delta^{13}C$ time series. Paleoceanography 21, 251–266.

Zachos, J.C., Flower, B.P., Paul, H., 1997. Orbitally paced climate oscillations across the Oligocene/Miocene boundary. Nature 388, 567–571.